Vol. **109** (2006) *ACTA PHYSICA POLONICA A* No. 4–5

Proceedings of the XI National School "Collective Phenomena and Their Competition"
Kazimierz Dolny, September 25–29, 2005

XANES Study of $La_{0.75-x}Gd_xCa_{0.25}MnO_{3-\delta}$ Solid Solutions

V.A. Drozd[a,c], M. Pękała[b], R.S. Liu[c], J.-F. Lee[d] and J.M. Chen[d]

[a]Department of Chemistry, Kiev National Taras Shevchenko University
60 Volodymyrska, Kiev, 01033 Ukraine
[b]Department of Chemistry, Warsaw University
Żwirki i Wigury 101, Warsaw, Poland
[c]Department of Chemistry, National Taiwan University
Roosevelt Road, Section 4, Taipei 106, Taiwan, ROC
[d]National Synchrotron Radiation Research Centre, Hsinchu 300, Taiwan, ROC

A series of solid solutions $La_{0.75-x}Gd_xCa_{0.25}MnO_{3-\delta}$ with $0.0 \leq x \leq 0.75$ was prepared via carbonate precursor precipitation method. Final sintering was performed at 1250°C in oxygen flow atmosphere. The samples obtained were characterized by scanning electron microscope, X-ray diffraction measurements. Oxygen stoichiometry was analyzed by iodometric titration method. X-ray absorption spectroscopic methods of Mn L-edge and Mn K-edge X-ray absorption near edge structure were used to study oxidation state of manganese in the solid solutions and elucidate features of their local crystal structure. Orthorhombic crystal structure characteristics of the solid solutions were refined by Rietveld method. An increase in oxygen deficiency and average manganese oxidation state were found to accompany Gd concentration increase in $La_{0.75-x}Gd_xCa_{0.25}MnO_{3-\delta}$. These results are consistent with Mn L-edge X-ray absorption near edge structure spectra, where a gradual change of Mn oxidation state with Gd concentration increase was detected. Origins of oxygen deficiency $La_{0.75-x}Gd_xCa_{0.25}MnO_{3-\delta}$ are discussed in terms of structural disorder caused by Gd substitution for La.

PACS numbers: 75.47.Lx, 61.10.Ht

1. Introduction

Mixed-valence manganites $RE/La_{1-x}Ca_xMnO_3$ with a perovskite structure exhibit a rich phase diagram and the strong interplay between structure, magnetic,

and transport properties [1–4]. The substitution of La atoms by the smaller Gd ones retains the doping level while it distorts the lattice varying the Mn–O–Mn bonding angle. The present paper is aimed at an investigation of the gadolinium substituted manganites $La_{0.75-x}Gd_xCa_{0.25}MnO_3$ by the X-ray absorption spectroscopy methods.

2. Experimental

A series of manganites $La_{0.75-x}Gd_xCa_{0.25}MnO_{3-\delta}$ ($x = 0$, 0.25, 0.50, 0.75) was prepared via carbonates precursor method using ammonium carbonate, $(NH_4)_2CO_3$, as the precipitator [2–5]. Carbonate precipitates were converted to $La_{0.75-x}Gd_xCa_{0.25}MnO_{3-\delta}$ solid solutions by slowly heating in the air atmosphere up to 810°C with the subsequent annealing at this temperature for several hours. Then the powders were grinded in an agate mortar and annealed at 900°C for 24 hours. Finally, they were grinded again, pressed into pellets and annealed at 1250°C for 48 h in a flowing oxygen atmosphere.

The samples obtained were characterized by X-ray diffraction (XRD) analysis using a SCITAG (X1) diffractometer with Cu K_α radiation. The diffraction intensity was measured from 10 to 120° with a step of 0.02° and a counting time of 10 s per step. The crystal structure was refined by Rietveld method using GSAS (general structure analysis system) program package.

The oxygen content of the $La_{0.75-x}RE_xCa_{0.25}MnO_{3-\delta}$ samples was determined by the iodometric titration assuming that the samples have initial cation stoichiometry.

Synchrotron radiation based experiments were performed in National Synchrotron Radiation Centre (NSRRC) in Taiwan. The electron storage ring was operated at an energy of 1.5 GeV with a beam current of 100–200 mA. The Mn K-edge X-ray absorption near edge structure (XANES) spectra were performed at the BL17C Wiggler beamline. A Si(111) double-crystal monochromator was used for energy selection with a resolution ($\Delta E/E$) of about 2×10^{-4}. The XANES spectra at the Mn K-edge were recorded at room temperature in transmission mode using gas-filled ionization chambers to measure the intensities of the incident (I_0), transmitted (I_t), and reference (I_{ref}) signals. A 7 μm thick iron foil was used as a reference. Both Fe foil and I_{ref} detector were positioned downstream the sample along the X-ray beam direction. The data from 3 scans were averaged, and the background was subtracted. The XANES spectra were normalised with respect to the edge jump step.

The Mn L-edge XANES measurements were performed on the BL20A high-energy spherical grating monochromator (HSGM) beamline in electron-yield mode. Simultaneously to electron-yield, the incident photon flux was monitored by a Ni mesh located after the exit slit of the monochromator. The photon energies were calibrated with an accuracy of 0.1 eV using the known O K-edge absorption peaks of a CuO compound. The X-ray fluorescence-yield absorption spectra were normalized to I_0.

3. Structural characterization

All samples studied by powder X-ray diffraction method are single phase. Their XRD patterns were indexed in orthorhombic space group *Pbnm*. GSAS program was used for Rietveld refinement of the structural parameters. The results of this refinement are summarized in Table. Figure 1 shows a typical XRD diffraction pattern of the system studied together with the results of the fitting. Crystal lattice parameters a and c as well as unit cell volume decrease with increasing gadolinium content that is caused by the difference in ionic radii of lanthanum

TABLE

Atomic positions, isotropic thermal factors (B), reliability factors, selected interatomic distances, and bond angles for the refinement of $La_{0.75-x}Gd_xCa_{0.25}MnO_{3-\delta}$ solid solutions in the space group *Pbnm* from XRD data at 300 K. Reflections (121) or (111) of the space group *Pbnm* are considered as preferred orientation (P.O.). R_P and R_{WP} are fitting correlation factors.

	$x = 0$	$x = 0.33$	$x = 0.75$
a/Å	5.4733(2)	5.42638(6)	5.3317(1)
b/Å	5.4631(2)	5.50137(6)	5.5998(1)
c/Å	7.7424(3)	7.67130(8)	7.5021(1)
V/Å^3	231.51(2)	229.008(4)	223.982(7)
x(La, Gd, Ca)	0.9997(7)	0.9935(2)	0.98640(2)
y(La, Gd, Ca)	0.0190(2)	0.03895(7)	0.0621(1)
B(La, Gd, Ca)/L'^2	0.583(9)	0.620(8)	0.369(12)
B(Mn)/L'^2	0.17(2)	0.083(17)	0.097(32)
x[O(1)]	0.049(2)	0.0811(9)	0.091(1)
y[O(1)]	0.4955(9)	0.4852(6)	0.4705(9)
B[O(1)]/L'^2	0.07(2)	0.63(14)	0.29(17)
x[O(2)]	0.723(1)	0.7178(7)	0.7073(8)
y[O(2)]	0.2676(1)	0.2899(6)	0.3088(8)
z[O(2)]	0.0415(9)	0.0377(4)	0.0461(6)
B[O(2)]/L'^2	0.94(11)	0.52(9)	1.06(13)
Mn–O1(axial)/L'^2	1.95392(8)	1.96942(2)	1.94384(3)
Mn–O2(equatorial)/Å	2.00319(7)	2.00614(2)	2.08135(3)
Mn–O2/L'	1.93146(5)	1.94028(2)	1.92366(2)
Mn–O1–Mn	164.293(1)	153.713	149.528(1)
Mn–O2–Mn	158.652(1)	156.485(0)	149.697(0)
P.O. (hkl)	1.255(111)	1.055(121)	1.132(111), 1.182(121)
χ^2	0.6590	0.4334	1.250
R_P(%)	5.22	4.05	5.69
R_{WP}(%)	7.48	5.29	7.84

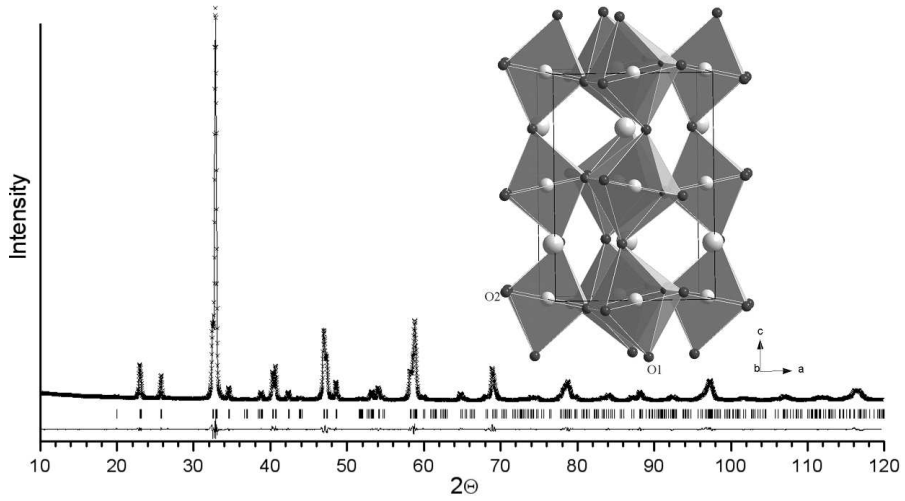

Fig. 1. Results of Rietveld refinement of $La_{0.25}Gd_{0.50}Ca_{0.25}MnO_{3-\delta}$. The inset shows crystal structure of the same compound.

and gadolinium. The value of Mn–O–Mn angle, which is considered to affect the degree of manganese and oxygen orbitals, decreases too with an x increase.

Figure 2 shows microphotographs of the synthesized $La_{0.75-x}Gd_xCa_{0.25}MnO_3$ solid solutions with $x = 0$ and 0.50. The average particle size estimated by scanning electron microscope (SEM) is less than 1 μm. It demonstrates a small increase with x as it is seen in Fig. 2. This growth could be explained by a decrease in melting temperature of the solid solutions with Gd concentration increase. In this case the grain growth rate should by higher for the compositions with a higher gadolinium content.

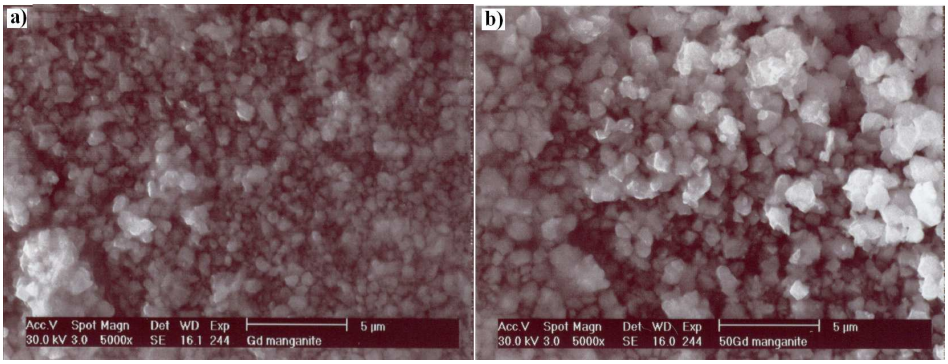

Fig. 2. SEM micrographs of $La_{0.75}Ca_{0.25}MnO_3$ (a) and $La_{0.25}Gd_{0.50}Ca_{0.25}MnO_3$ (b).

According to the results of iodometric titration the systematic decrease in total oxygen content was observed, which is illustrated in Fig. 3. Subsequently,

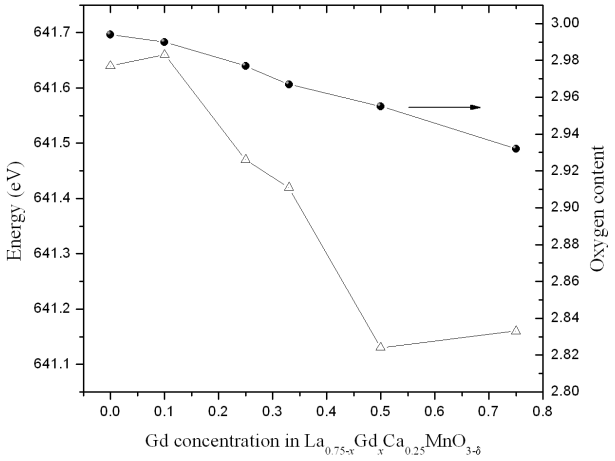

Fig. 3. Total oxygen content and energy position of Mn L_3 peak as functions of Gd concentration.

also the average manganese oxidation state decreases with Gd concentration increase.

4. XANES results

The Mn L-edge XANES of $La_{0.75-x}Gd_xCa_{0.25}MnO_3$ solid solutions and standards measured in electron-yield mode are shown in Fig. 4. The shift of Mn L_3 Mn L_2 peak position to high energies with Gd content increase indicates a decrease of Mn oxidation state in the solid solutions. This observation is in good agreement with the results of iodometric titration which lead to the similar conclusions

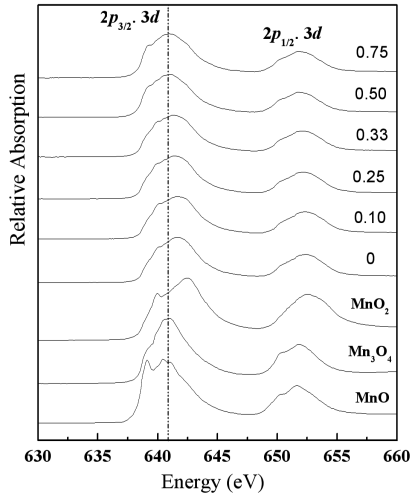

Fig. 4. XANES Mn L-egde spectra of $La_{0.75-x}Gd_xCa_{0.25}MnO_3$ solid solutions.

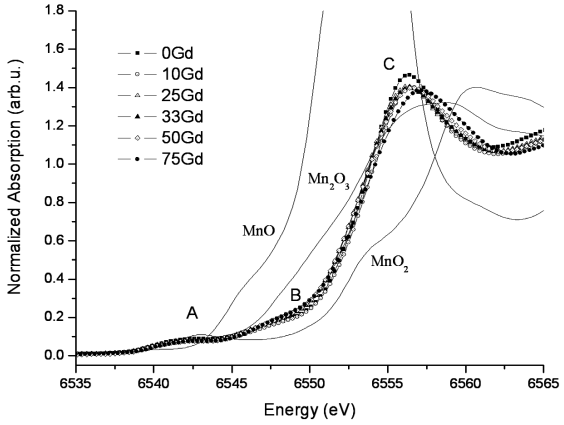

Fig. 5. XANES Mn K-egde spectra of $La_{0.75-x}Gd_xCa_{0.25}MnO_3$ solid solutions and standards manganese oxides. A, B, and C mark energy regions.

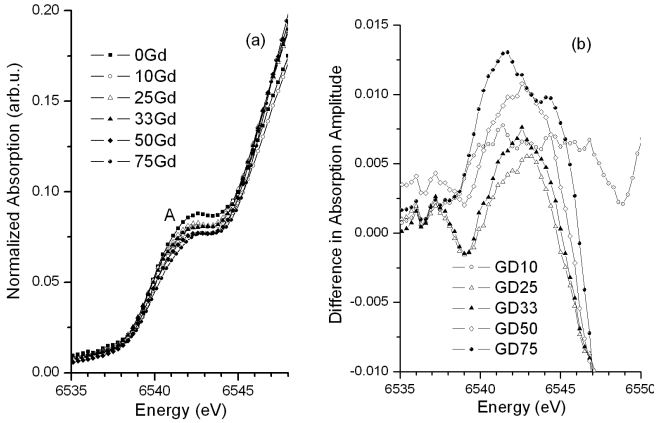

Fig. 6. Pre-edge region of Mn K-edge XANES of $La_{0.75-x}Gd_xCa_{0.25}MnO_3$ solid solutions (a) and the difference spectra of the same region (b): [Data($La_{0.75}Ca_{0.25}MnO_3$) − Data($La_{0.75-x}Gd_xCa_{0.25}MnO_3$)].

(Fig. 3). In Fig. 5 the evolution with x XANES Mn K-edge spectra are shown. Pre-edge feature A is ascribed to $1s-3d$ transition. The amplitude of this peak usually is associated with increasing hole concentration in $3d$ transition-metals orbitals. Enhancement of this feature with an x increase is evident from Fig. 6 where pre-edge region is shown in an enlarge scale together with difference spectra.

Surprisingly, unlike to XANES Mn L-edge spectra, peak positions in Mn K-edge spectra do not change significantly with x variations in $La_{0.75-x}Gd_xCa_{0.25}MnO_3$ solid solutions. Mn L-edge XANES were measured in electron-yield mode while K-edge XANES measurements were carried out in trans-

mission mode. The latter technique gives information only about the thin surface layer of $\sim$ 50 Å while the former one characterizes bulk properties of the material. Thus, the difference between trends observed by Mn L- and K-edges XANES spectra can be caused by inhomogeneous distribution of oxygen vacancies through the depth in $La_{0.75-x}Gd_xCa_{0.25}MnO_3$ particles. Therefore, the oxygen vacancies have a higher concentration on the surface of the particles.

The Fourier transforms of the EXAFS Mn K-edge experimental signal of $La_{0.75-x}Gd_xCa_{0.25}MnO_3$ solid solutions allow distinguishing four coordination shells of Mn atoms. The first octahedral coordination shell (Mn–O) is only weakly affected by the Gd substitution as the first peak shifts less than 0.05 Å. A location of the second peak shifts to lower R values by about 0.2 Å and proves that the second coordination shell (Mn–Gd/La/Ca) shrinks gradually with raising Gd content [6, 7].

5. Conclusions

The substitution of La atoms by the Gd ones varies the local coordination shells of Mn ions and causes an increase in oxygen deficiency and average manganese oxidation in $La_{0.75-x}Gd_xCa_{0.25}MnO_3$ systems. These results are consistent with Mn L-edge XANES spectra, where a gradual change of Mn oxidation state with Gd concentration increase is detected. The origin of oxygen deficiency $La_{0.75-x}Gd_xCa_{0.25}MnO_3$ is related to structural disorder caused by Gd substitution for La. An influence of Gd doping on magnetic and transport properties of this family of manganites is reported separately [8].

Acknowledgment

The work was supported in parts by PST.MEM.CLG.980654, Polish–Belgian Scientific Exchange Program and Scientific Network "Oxide Materials with Highly Correlated Electrons" and Kasa Mianowskiego.

References

[1] L.P. Gorkov, V.Z. Kresin, *Phys. Rep.* **400**, 149 (2004).

[2] T.L. Aselage, D. Emin, S.S. McCready, E.L. Venturini, M.A. Rodriguez, J.A. Voigt, T.J. Headley, *Phys. Rev. B* **68**, 134448 (2003).

[3] V. Drozd, M. Pękała, J. Kovac, I. Skorvanek, *Czechosl. J. Phys.* **54**, Suppl. D, D415 (2004).

[4] G.F. Snyder, C.H. Booth, F. Bridges, R. Hiskes, S. DiCarolis, M.R. Beasley, T.H. Geballe, *Phys. Rev. B* **55**, 6453 (1997).

[5] V. Drozd, M. Pękała, J. Kovac, I. Skorvanek, S. Nedilko, *Acta Phys. Pol. A* **106**, 751 (2004).

[6] C. Castellano, F. Cordero, O. Palumbo, R. Cantelli, R. Cimberle, M. Tropeano, A. Martinelli, M. Ferretti, *Solid State Commun.* **136**, 244 (2005).

[7] M. Croft, D. Sills, M. Greenblatt, C. Lee, K.V. Ramanujachary, D. Tran, *Phys. Rev. B* **55**, 8726 (1997).

[8] M. Pękała, V.A. Drozd, to be submitted to *Acta Phys. Pol. A*.